Magnetization Plateaus and Thermal Entanglement of Spin Systems

N Ananikian[1], Č Burdík [2], L Ananikyan [1] and H Poghosyan[1]

[1] Theory Department , A.I. Alikhanyan National Science Laboratory, 0036 Yerevan, Armenia
[2] Department of Mathematics, Czech Technical University, Prague 12000, Czech Republic

E-mail: ananik@yerphi.am

Abstract. The geometrically magnetic frustrations and quantum thermal entanglement of antiferromagnetic metal-containing compounds are considered on a diamond chain. We researched the magnetic and thermal properties of the symmetric Hubbard dimers with delocalized interstitial spins and the quantum entanglement states. It is presented magnetization plateaus and negativity in spin-1 Ising-Heisenberg model using transfer matrix technique. Applying the dynamic system approach we study the magnetic curves, Lyapunov exponents and superstable point in the two-dimensional mapping for the partition function of spin-1 classical and Ising-Heisenberg models at $T \to 0$ on a diamond chain.

1. Introduction

The magnetic plateau and entanglement properties exhibit common features observable via antiferromagnetic coupling constant, external magnetic, crystal (single-ion anisotropy) fields and chemical potential. The family of known non-trivial quantum effects in the condensed matter physics is enriched with the novel phenomenonintermediate plateaus in the magnetization processes [1, 2]. The observation of a 1/3 magnetization plateau in natural azurite $Cu_3(CO_3)_2(OH)_2$ has been proposed as a realization of the exotic diamond chain of antiferromagnetically coupled spin-1/2 Cu^{+2}-monomers [3, 4]. The theoretical study of magnetization plateaus in azurite were obtained by using the density functional theory [5, 6], mean-field-like treatment based on the Gibbs-Bogoliubov inequality [7] , the density-matrix renormalization-group (DMRG) technique [8,9] and the decoration-iteration transformation [10]. On a diamond chain there were observed the plateaus of electron density as a function of chemical potential on spinless fermion, extended Hubbard and magnetization as a function of external magnetic field on distorted Ising-Hubbard models [11–13]. The magnetic behavior and magnetic susceptibility of the metal-containing complex $[Ni_3(fum)_2 - (\mu_3 - OH)_2(H_2O)_4]_n \cdot (2H_2O)_n$ was measured [14]. The spin-1 diamond-chain of the compound is characterized by both ferromagnetic and antiferromagnetic exchanges. In this article we would get magnetization and quadrupole moment plateaus at low temperatures as a function of external magnetic field and single-ion anisotropy. Quantum entanglement is considered to play a key role for understanding of strongly correlated quantum systems, quantum phase transitions and collective quantum phenomena in particular many-body spin and fermionic lattice systems [15–17] especially in antiferromagnetic models. Another important observation is the strong relationship between magnetic and entanglement properties of the antiferromagnetic system on diamond chain models

[18–25]. We also considered magnetic behavior of spin lattice models applying the dynamic system method [26–28]. The dynamical approach represents an essential tool in the theory of phase transitions and criticality and it enhanced our understanding of the phase structure and critical properties of spin models. In the case of antiferromagnetic coupling between lattice nodes of the three site interaction Ising and the Q-state Potts models ($Q < 2$) on Husimi and Bethe lattices exhibit a complex behavior, featuring doubling bifurcations, chaotic regimes, intermittency, and superstable points [29,30]. The plateaus of the maximal Lyapunov exponent coincide with magnetization plateaus on a kagome chain for multidimensional mapping [31]. The existence of magnetization plateau has been observed at one third of the saturation magnetization in the antiferromagnetic spin-1/2 IsingHeisenberg model on a diamond chain using the multidimensional mapping [32]. It has been detected that the maximal Lyapunov exponent exhibits plateau like magnetization one and found the existence of the supercritical point at $T \to 0$ in the absence of the external magnetic field corresponding to phase transition point.

In the present paper we mainly deal with the quantum entanglement and magnetic curve behavior of symmetric Hubbard dimers with delocalized interstitial electrons and spin-1 Ising - Heisenberg model using transfer matrix technique on a diamond chain. Applying the recurrence relation of the two-dimensional mapping we study magnetic plateau and their relation to maximal Lyapunov exponents, superstable point of spin-1 classical and Ising - Heisenberg models on a diamond chain. The paper is organized as follows. In Section 2 the phase behavior of the diamond chain is presented of a symmetric Hubbard-Ising model and studied the magnetic and thermal properties. We researched the quantum entanglement of electrons in Hubbard dimers and dependence of Hamiltonian parameters as well as on temperature. We give an exact solution of spin-1 Ising - Heisenberg model by means of the transfer-matrix method and study the magnetization plateaus and negativity in Section 3. In Section 4 we apply the dynamical system approach in researching magnetic plateaus and maximal Lyapunov exponent plateaus. It is observed that the superstable coincide with phase transition point at $T \to 0$ in the spin-1 classical and Ising-Heisenberg models on the diamond chain. Some concluding remarks are given in section 5.

2. Symmetric diamond chain with delocalized Hubbard interstitial spins

The Hamiltonian of symmetric Ising- Hubbard model [33] describing the diamond chain (Fig. 1)is

$$\mathcal{H} = \sum_{i=1}^{N} \mathcal{H}_{i,i+1}, \text{ where}$$

$$\mathcal{H}_{i,i+1} = -\tilde{t}\left(a_{i\uparrow}^{+}b_{i\uparrow} + a_{i\uparrow}b_{i\uparrow}^{+} + a_{i\downarrow}^{+}b_{i\downarrow} + a_{i\downarrow}b_{i\downarrow}^{+}\right) + \widetilde{V}n_{ai}n_{bi} + \widetilde{U}\left(n_{ai\uparrow}n_{ai\downarrow} + n_{bi\uparrow}n_{bi\downarrow}\right) \quad (1)$$

$$+\widetilde{J}_m s_{ci}s_{ci+1} + J\left(s_{ai}^{z} + s_{bi}^{z}\right)\left(s_{ci} + s_{ci+1}\right) - \widetilde{\mu}\left(n_{ai} + n_{bi}\right) - \widetilde{h}\left(s_{ai}^{z} + s_{bi}^{z} + \frac{s_{ci} + s_{ci+1}}{2}\right).$$

Here $a_{i\sigma}^{+}$ ($a_{i\sigma}$) and $b_{i\sigma}^{+}$ ($b_{i\sigma}$) are the electron creation (annihilation) operators with the spin value σ=($\uparrow,\downarrow$), respectively on sites a_i and b_i. The $n_{ai\sigma} = a_{i\sigma}^{+}a_{i\sigma}$ and $n_{bi\sigma} = b_{i\sigma}^{+}b_{i\sigma}$ are the electron number operators, respectively on sites a_i and b_i and t is the hopping amplitude. We denote $n_{\alpha i} = n_{\alpha i\uparrow} + n_{\alpha i\downarrow}$, $s_{\alpha i}^{z} = \frac{1}{2}\left(n_{\alpha i\uparrow} - n_{\alpha i\downarrow}\right)$, ($\alpha = a, b$) and $s_{ci} = \pm\frac{1}{2}$. Here $\tilde{\mu}$ and $\widetilde{h}$ are the values of the chemical potential and the external magnetic field ($\widetilde{h} = g\mu_B B_z$) respectively. The terms which contain $\widetilde{U}$ and $\widetilde{V}$ correspond respectively to one–site and two–site Coulomb repulsions in the Hubbard dimer(interstitial spins). The terms which contain the symmetric coupling J that describe Hubbard dimer interactions with nodal Ising-type spins. The term containing $\widetilde{J}_m$ describes two nodal Ising–like spins interaction.

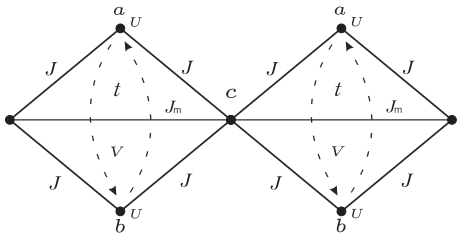

Figure 1. Two sites of the Hubbard dimer are denoted as a– and b–. There is an electron hopping between them with amplitude t. One–site (U) and two–site (V) Coulomb interactions are also present. The diamonds are connected to each other at nodal c–sites. There is an Ising–like direct interaction with J_m coupling constant between the nodal sites. The nodal sites are also connected to a– and b–sites by means of Ising–like interactions with coupling constant J.

From the identity

$$\widetilde{V} n_a n_b + \widetilde{U} \left(n_{a\uparrow} n_{a\downarrow} + n_{b\uparrow} n_{b\downarrow} \right) = \left(\widetilde{U} - \widetilde{V} \right) \left(n_{a\uparrow} n_{a\downarrow} + n_{b\uparrow} n_{b\downarrow} \right) + \frac{n\left(n-1\right)}{2} \widetilde{V}, \tag{2}$$

(where $n = n_{a\uparrow} + n_{a\downarrow} + n_{b\uparrow} + n_{b\downarrow}$ is the total number of electrons in the Hubbard dimer), it follows that the differences between energy levels depend on $\widetilde{U} - \widetilde{V} \equiv \widetilde{W}$ only, if n is fixed. In particular, for fixed $n \neq 2$, $\left(n_{a\uparrow} n_{a\downarrow} + n_{b\uparrow} n_{b\downarrow} \right)$ is constant and the behavior of the system does not depend on $\widetilde{W}$ at all, which is physically obvious.

As all $\mathcal{H}_{i,i+1}$ commute, therefore the partition function can be written as:

$$Z_N = Tr\left(e^{-\beta \mathcal{H}} \right) \;\; = \;\; \sum_{s_{ci} = \pm \frac{1}{2}} \prod_{i=1}^{N} Tr_{a,b} \left(e^{-\beta \mathcal{H}_{i,i+1}(s_{ci}, s_{ci+1})} \right) = Tr \mathbf{V}^N, \tag{3}$$

where $\mathbf{V} = \begin{pmatrix} V(+,+) & V(+,-) \\ V(-,+) & V(-,-) \end{pmatrix}$ is the transfer matrix, with $V\left(\pm,\pm\right) = \sum\limits_j e^{-\beta E_j(\pm,\pm)}$, where $E_j\left(\pm,\pm\right) \equiv E_j\left(\pm\frac{1}{2},\pm\frac{1}{2}\right)$ are the eigenvalues of the $\mathcal{H}_{i,i+1}\left(\pm,\pm\right) \equiv \mathcal{H}_{i,i+1}\left(\pm\frac{1}{2},\pm\frac{1}{2}\right)$ Hamiltonian.

In the thermodynamic limit the free energy per diamond is

$$F = \lim_{N\to\infty} \frac{-T}{N} \ln Z_N = -\ln \lambda_1, \tag{4}$$

where $\lambda_1 = \frac{1}{2}\left(Tr\mathbf{V} + \sqrt{\left(Tr\mathbf{V}\right)^2 - 4 \det \mathbf{V}} \right)$ is the largest eigenvalue of the transfer matrix.

On this basis it is easy to calculate magnetization and specific heat. Analogously we use the following expression for reduced density matrix of a Hubbard dimer to study entanglement properties:

$$\begin{aligned} \rho' \;\; &= \;\; \frac{1}{\lambda_1} \left[\frac{e^{-\beta H(+,+)} + e^{-\beta H(-,-)}}{2} + e^{-\beta H(+,-)} \sin 2\theta \; + \right. \\ &+ \;\; \left. \frac{e^{-\beta H(+,+)} - e^{-\beta H(-,-)}}{2} \cos 2\theta \right], \end{aligned} \tag{5}$$

with $\sin 2\theta = \dfrac{2V\left(+,-\right)}{\sqrt{\left(Tr\mathbf{V}\right)^2 - 4\det\mathbf{V}}}$, $\cos 2\theta = \dfrac{V\left(+,+\right) - V\left(-,-\right)}{\sqrt{\left(Tr\mathbf{V}\right)^2 - 4\det\mathbf{V}}}$.

In the sequel we rescale all quantities by the J absolute value, substituting $t = \tilde{t}/|J|$, $h = \tilde{h}/|J|$, $\mu = \tilde{\mu}/|J|$, $U = \widetilde{U}/|J|$, $V = \widetilde{V}/|J|$, $W = \widetilde{W}/|J|$ and $J_m = \tilde{J}_m/|J|$.
The magnetization curves at nonzero temperature are derived from $m = -\frac{\partial F}{\partial h}$. Here we take the number of electrons in a Hubbard dimer fixed and equals to 2. Fig. 2 shows possible forms of magnetization curves at zero and nonzero temperatures. The following types of plateaus exist here: at 0, 1/3 and 2/3 values and of classical (electrons in the Hubbard dimers are not entangled and their spin projections have definite value at each site) and non-classical (electrons in the Hubbard dimers are entangled) types.

The entanglement of formation in the special case of two spin-1/2 particles has the analytical expression [35]: $E_F = H\left(\frac{1+\sqrt{1-C^2}}{2}\right)$, where $H(x) = -x\log_2(x) - (1-x)\log_2(1-x)$, and C is the quantity called *concurrence*. For fixed values of t and J_m we have plotted the concurrence as a function of the temperature and the external magnetic field (Figs. 3). The thermal entanglement becomes significantly large when the energy level of the (non-entangled) ground state and the nearest energy level (corresponding to the entangled state) are close to each other.

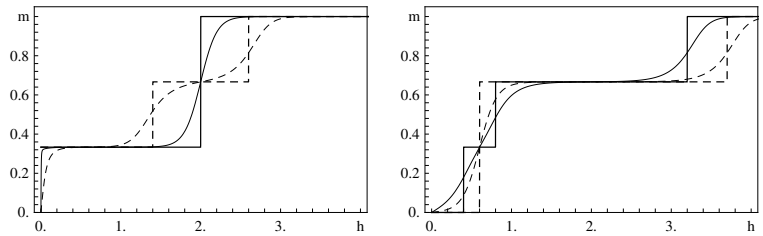

Figure 2. Dependence of the diamond chain magnetization (m) (per diamond in $g\mu_B$ units) on the external magnetic field (h) for different values of the internodal change interaction (J_m) at $T = 0$. The fixed chain parameters are $t = 0.3$, $W = 0$, $\mu = 0$. The case of $T = 0.1$ is also shown. Thermal fluctuations smoothen magnetization jumps. Bold lines represent at $T = 0$ and solid, dashed lines represent the different values of J_m accordingly.

3. Magnetization plateaus and negativity in spin-1 Ising - Heisenberg model

Let us consider spin-1 Ising-Heisenberg model on a diamond chain (see Fig. 6) without biquadratic coupling terms using the transfer matrix technique. The magnetic behavior of homometallic molecular ferrimagnet $[Ni_3(fum)_2 - (\mu_3 - OH)_2(H_2O)_4]_n \cdot (2H_2O)_n$ was measured by [14] without single-ion anisotropy parameters. We observe magnetization plateau and thermal quantum negativity in the presence of an external magnetic fields and single-ion anisotropy terms. The Hamiltonian is equal to the sum over block Hamiltonians $\mathcal{H} = \sum_i \mathcal{H}_i$ with

$$\begin{aligned}\mathcal{H}_i &= J\vec{S}_{a,i}\vec{S}_{b,i} + J_1(S^z_{a,i} + S^z_{b,i})(\sigma^z_i + \sigma^z_{i+1}) + D_H((S^z_{a,i})^2 + (S^z_{b,i})^2) + \frac{D_I}{2}\left((\sigma^z_i)^2 + (\sigma^z_{i+1})^2\right) \quad (6)\\ &- h_H g\mu_B(S^z_{a,i} + S^z_{b,i}) - \frac{h_I g\mu_B}{2}\left(\sigma^z_i + \sigma^z_{i+1}\right),\end{aligned}$$

where $S^{\alpha}_{a/b,i}$ ($\alpha = x, y, z$) are spin-1 operators on the sites with coordinates $(a/b, i)$, while σ^z_i's are z projections of spin-1 operator resting on the sites i, J denotes the XXX interaction within the Heisenberg dimer and J_1 stands for the interaction between nodal and dimer spins. Coefficients

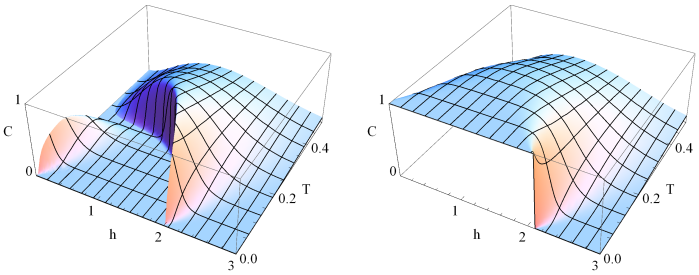

a) $t = 0.45, J_m = -2$ b) $t = 0.55, J_m = -2$

Figure 3. The dependence of the concurrence from temperature and external magnetic field for various values of hopping amplitude. Concurrence vanishes in high temperature limit.

D_I and D_H correspond to the longitudinal crystal(single-ion anisotropy) fields in the z direction. The gyromagnetic ratio is taken to be $g = 2.2$ in the plots drawn below, which is more or less typical for nickel containing compounds. We assume that cyclic boundary condition $\sigma_{N+1} = \sigma_1$ is applied. The block Hamiltonians($\mathcal{H}_i$) are commutative, therefore the partition function can be written like in equation (3).

After direct diagonalization of the block Hamiltonian $\mathcal{H}_i$ one gets the energy spectrum of a diamond block depending on Ising spins:

$$\begin{aligned}
E_1 &= -J - \frac{h_I g\mu_B}{2}(\sigma_i + \sigma_{i+1}) + \frac{D_I}{2}\left(\sigma_i^2 + \sigma_{i+1}^2\right) + 2D_H, \\
E_{2,3} &= \pm J - \left(J_1 + \frac{h_I g\mu_B}{2}\right)(\sigma_i + \sigma_{i+1}) + h_H g\mu_B + D_H + \frac{D_I}{2}\left(\sigma_i^2 + \sigma_{i+1}^2\right), \\
E_{4,5} &= \pm J + (J_1 - \frac{h_I g\mu_B}{2})(\sigma_i + \sigma_{i+1}) - h_H g\mu_B + D_H + \frac{D_I}{2}\left(\sigma_i^2 + \sigma_{i+1}^2\right), \\
E_{6,7} &= J + \left(\pm 2J_1 - \frac{h_I g\mu_B}{2}\right)(\sigma_i + \sigma_{i+1}) \mp 2h_H g\mu_B + \frac{D_I}{2}\left(\sigma_i^2 + \sigma_{i+1}^2\right) + 2D_H, \\
E_{8,9} &= \frac{-J \pm \Lambda}{2} - \frac{h_I g\mu_B}{2}(\sigma_i + \sigma_{i+1}) + \frac{D_I}{2}\left(\sigma_i^2 + \sigma_{i+1}^2\right) + D_H,
\end{aligned} \tag{7}$$

where $\Lambda = \sqrt{(2D_H - J)^2 + 8J^2}$. Knowledge of the spectrum allows us to perform partial trace-overs along Heisenberg degrees of freedom. Which makes representation $Z_N = \sum_{\sigma_i} \prod_{i=1}^{N} V_{\sigma_i,\sigma_{i+1}}$, with $V_{\sigma_i,\sigma_{i+1}} = Tr_i e^{-\beta\mathcal{H}_i} = \sum_{i=1}^{9} e^{-\beta E_i(\sigma_i,\sigma_{i+1})}$. $V_{\sigma_i,\sigma_{i+1}}$'s may be viewed as components of a 3×3 transfer matrix:

$$V_{\sigma_i,\sigma_{i+1}} = \begin{pmatrix} V_{-1,-1} & V_{-1,0} & V_{-1,1} \\ V_{0,-1} & V_{0,0} & V_{0,1} \\ V_{1,-1} & V_{1,0} & V_{1,1} \end{pmatrix}, \tag{8}$$

where matrix indexes are the three possible projections of Ising spins. Taking into account the cyclic boundary conditions one may write $Z_N = Tr(V^N)$ in transfer matrix notations. Hence the partition function may be expressed in terms of the transfer matrix eigenvalues:

$$Z_N = \lambda_1^N + \lambda_2^N + \lambda_3^N. \tag{9}$$

As usual, in the thermodynamic limit $N \to \infty$ only the contribution of the largest eigenvalue must be considered. Denoting the maximal eigenvalue as λ, the free energy per block for infinitely long chain takes the form

$$f = -\frac{1}{\beta}\lim_{N\to\infty}\frac{1}{N}\ln Z_N = -\frac{1}{\beta}\ln\lambda. \tag{10}$$

The exact expression of the free energy will allow us to calculate thermodynamic quantities of the system. In the present paper we will consider the sublattice magnetization and quadrupole moment of Ising spins and the sublattice magnetization of Heisenberg spins. They are given by

$$m_I = -\frac{\partial f}{\partial h_I}, \quad m_H = -\frac{1}{2}\frac{\partial f}{\partial h_H}, \quad q_I = \frac{\partial f}{\partial D_I}. \tag{11}$$

The total magnetization is equal to the average of m_I and two m_H. To illustrate the magnetization process in a few interesting cases. We show the magnetization at sufficiently low temperature ($T = 0.01K$) as a function of the magnetic field with several plateaus (Fig. 4). Thermal quantum entanglement (negativity) can be defined as [36]. We have plotted negativity

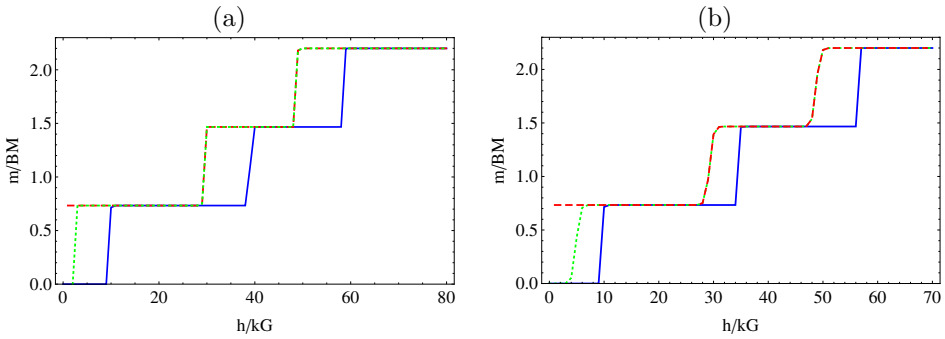

Figure 4. Low temperature ($T = 0.01K$) magnetization curves in Bohr magneton units when $J_1 = D_I = 1cm^{-1}$ and (a) $J = -6cm^{-1}$, $D_H = 1cm^{-1}$ (dashed), $D_H = 2.25cm^{-1}$ (dotted), $D_H = 4cm^{-1}$ (solid), (b) $J = 0.9cm^{-1}$, $D_H = -1cm^{-1}$ (dashed), $D_H = 0.7cm^{-1}$ (dotted), $D_H = 2cm^{-1}$ (solid).

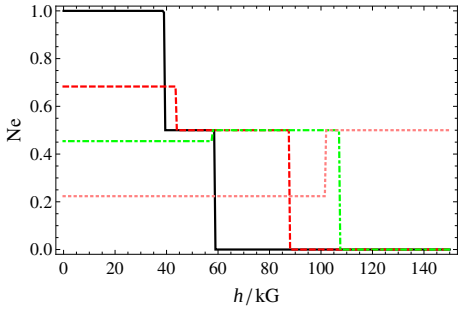

Figure 5. Negativity via magnetic field for different values of the single-ion anisotropy $D_H = 0, 3, 5, 10cm^{-1}$ (solid, dashed, dotted-dashed and dotted curves, respectively) at low temperature $T = 10^{-4}K$ and for $J = 2cm^{-1}$. Here $J_1 = D_I = 1cm^{-1}$.

vs. magnetic field Fig. 5(a) , demonstrating the change of negativity by varying D_H as well as the sharp step like behavior of the entanglement at transitions. The introduction of the single-ion anisotropy is essential for the observation of magnetic and entanglement properties for homometallic molecular ferrimagnet $[Ni_3(fum)_2 - (\mu_3 - OH)_2(H_2O)_4]_n \cdot (2H_2O)_n$.

4. Magnetic plateaus and quantum entanglement: Dynamical approach

In this section we utilise two models the spin-1 Ising and Ising-Heisenberg models. Let us first consider the spin-1 Ising model on diamond chain with free boundary conditions in the

presence of an external magnetic field (see Fig. 6). The Hamiltonian operator of the model is equal to the summation of the block Hamiltonians and can be written as

$$\mathcal{H} = \sum_{i}^{N} \mathcal{H}_i = \sum_{i}^{N} (J(S_{a,i}S_{b,i}) + K(S_{a,i}S_{b,i})^2 + J_1(\mu_i + \mu_{i+1})(S_{a,i} + S_{b,i}) \tag{12}$$
$$+K_1((\mu_i)^2 + (\mu_{i+1})^2)((S_{a,i})^2 + (S_{b,i})^2) + \Delta((S_{a,i})^2 + (S_{b,i})^2) + \Delta_1 \frac{(\mu_i)^2 + (\mu_{i+1})^2}{2}$$
$$-h_H(S_{a,i} + S_{b,i}) - h_I \frac{\mu_i + \mu_{i+1}}{2})$$

Where $S_{a,i}$, $S_{b,i}$ and μ_i, μ_{i+1} are classic Ising spins and can take the values $1, 0, -1$. The parameter J stands for the linear interactions between the nearest-neighboring $S_{a,i}-S_{b,i}$ elements and J_1 is the linear interactions parameter for nearest-neighboring $S-\mu$ elements ($S_{a,i}-\mu_i$, $S_{a,i}-\mu_{i+1}$, $S_{b,i}-\mu_i$, $S_{b,i}-\mu_{i+1}$). Analogously K and K_1 stand for the quadratic interactions. Δ and Δ_1 are the single-ion anisotropy parameters, h_I and h_H are contributions of a longitudinal external magnetic field interacting with the Ising spins ($S_{a,i}, S_{b,i}-h_H$ and μ_i-h_I).This notations are made to highlight the similarities between the spin-1 Ising and Ising-Heisenberg models. In our further calculations we will consider the case when $K = J$, $K_1 = J_1$, $\Delta = \Delta_1$, $h_H = h_I = h$. The partition function of the system with Hamiltonian (12) is

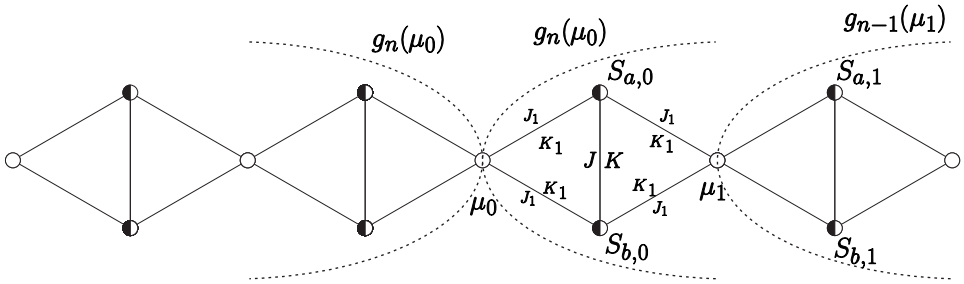

Figure 6. The procedure for derivation of the Ising (S_a and S_b are white) and Ising-Heisenberg (S_a and S_b are black) diamond chain. White circles are Ising spins and black are Heisenberg spins

$$Z = \sum_{\mu_i, S_{a,i}, S_{b,i}} \exp -\beta\mathcal{H} = \sum_{\mu_0} e^{-\frac{-h_I\mu_0 + \Delta_1\mu_0^2}{T}} g_n(\mu_0)^2 \tag{13}$$

where $\beta = (T)^{-1}$, T is the absolute temperature. By cutting diamond chain at μ_0 into two branches $g_n(\mu_0)$ (Fig. 1) the exact recursion relation for the partition function can be derived. The relation between $g_n(0)$ and $g_{n-1}(\mu_1)$ is given by the following equation.

$$g_n(\mu_0) = \sum_{\mu_1=-1}^{1} \sum_{S_{a,0}=-1}^{1} \sum_{S_{b,0}=-1}^{1} \exp[-\beta(J(S_{a,0}S_{b,0}) + K(S_{a,0}S_{b,0})^2 + J_1(\mu_1 + \mu_0)(S_{a,0} + S_{b,0}) + \tag{14}$$
$$K_1((S_{a,0}\mu_1)^2 + (S_{a,0}\mu_0)^2 + (S_{b,0}\mu_1)^2 + (S_{b,0}\mu_0)^2) + \Delta((S_{a,0})^2 + (S_{b,0})^2) + \Delta_1\mu_1^2$$
$$-h_H(S_{a,0} + S_{b,0}) - h_I\mu_1)] * g_{n-1}(\mu_1)$$

By introducing the following notation

$$x_n = \frac{g_n(1)}{g_n(0)}, \quad y_n = \frac{g_n(-1)}{g_n(0)} \tag{15}$$

we can get two-dimensional recursion relation for the partition function

$$\begin{aligned} x_n &= f1(x_{n-1}, y_{n-1}), \quad f_1(x,y) = \frac{a_1 + a_{11}x + a_{12}y}{b_0 + b_1 x + b_2 y} \\ y_n &= f2(x_{n-1}, y_{n-1}), \quad f_2(x,y) = \frac{a_2 + a_{21}x + a_{22}y}{b_0 + b_1 x + b_2 y} \end{aligned} \tag{16}$$

where the coefficients are easily calculated from equations (14) and (15).

Recursion relation (16) plays a crucial role in our further investigation because the order parameters magnetic and quadrupole moments can be expressed through two-dimensional rational mapping. The equations for total magnetic and quadrupole moments are expressed similar as [34].

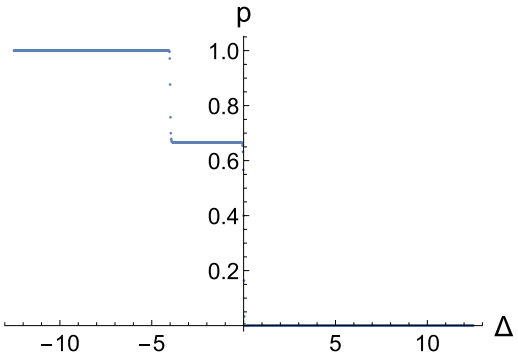

Figure 7. Classical Ising spin-1 quadrupole moment(p) for $J = 2, J_1 = 1, h = 0, T = 0.01$.

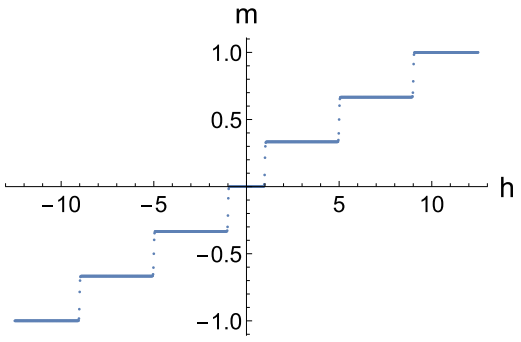

Figure 8. Classical Ising spin-1 magnetic moment(m) for $J = 2, J_1 = 1, \Delta = 1, T = 0.01$.

Now lets discus the spin-1 Ising-Heisenberg model on diamond chain with free boundary conditions in the presence of an external magnetic and crystal(single-ion anisotropy) fields (see Fig. 6). This two models are very similar therefore this time our narration will be more concise. The blocks of the diamond chain consist of two Heisenberg interstitial spins ($S^{\alpha}_{a,i}$ and $S^{\alpha}_{b,i}$). The z components of interstitial spins are coupled with nearest-neighboring nodal Ising spins (μ_i and μ_{i+1}). Like in the previous model the Hamiltonian of the system may be represented as a sum over block Hamiltonians

$$\begin{aligned} \mathcal{H} = \sum_i^N \mathcal{H}_i = \sum_i^N (J(S^x_{a,i}S^x_{b,i} + S^y_{a,i}S^y_{b,i} + DS^z_{a,i}S^z_{b,i}) + K(S^x_{a,i}S^x_{b,i} + S^y_{a,i}S^y_{b,i} + D_1 S^z_{a,i}S^z_{b,i})^2 \\ + J_1(\mu^z_i + \mu^z_{i+1})(S^z_{a,i} + S^z_{b,i}) + K_1((\mu^z_i)^2 + (\mu^z_{i+1})^2)((S^z_{a,i})^2 + (S^z_{b,i})^2) + \Delta((S^z_{a,i})^2 + (S^z_{b,i})^2) \\ + \Delta_1 \frac{(\mu^z_i)^2 + (\mu^z_{i+1})^2}{2} - h_H(S^z_{a,i} + S^z_{b,i}) - h_I \frac{\mu^z_i + \mu^z_{i+1}}{2}) \end{aligned} \tag{17}$$

In this equation, $S^{\alpha}_{a,i}$, $S^{\alpha}_{b,i}$ ($\alpha = x, y, z$) and μ^z_i represent relevant components of Heisenberg and Ising spin-1 operators. In equation (17) J is the linear Heisenberg interaction term, K is the

quadratic interaction term parameter, D and D_1 are anisotropy parameters, J_1 is the interaction parameter between the nearest-neighboring Ising and Heisenberg spins, Δ (Δ_1) is the single-ion anisotropy parameter of Heisenberg (Ising) spins and the parameter K_1 is the analogue of a quadratic Ising interaction term. The last two terms in the Hamiltonian are contributions of a longitudinal external magnetic field interacting with the Heisenberg and Ising spins. It is important to notice that the commutation relation between different block Hamiltonians is zero ($[H_i, H_j] = 0$). Furthermore it can be shown that the block Hamiltonian commutes with Ising and Heisenberg spins, i.e. $[H_i, \mu_i^z] = [H_i, S_{a,i}^z + S_{b,i}^z]$ for any values of the model parameters J , K , J_1, K_1, D, D_1, Δ, Δ_1 and magnetic field, but the block Hamiltonian and quadrupole moment commute,$[H_i, (S_{a,i}^z)^2 + (S_{b,i}^z)^2] = 0$, only when $J = KD_1$. In the present work we consider only the case when $J = K$, $J_1 = K_1$, $D = D_1 = 1$, $\Delta = \Delta_1$, $h_H = h_I = h$. Equation (2) and (3) are conserved for this model if instead of μ_i we insert μ_i^z considering the fact that here we also cut the diamond chain at μ_0 (see Fig. 6). From them its easy to calculate the equivalent of equation (14)

$$g_n(\mu_0) = \sum_{\mu_1, S_{a,0}, S_{b,0}} \exp[-\beta(J(S_{a,0}^x S_{b,0}^x + S_{a,0}^y S_{b,0}^y + D S_{a,0}^z S_{b,0}^z) + K(S_{a,0}^x S_{b,0}^x + S_{a,0}^y S_{b,0}^y + D_1 S_{a,0}^z S_{b,0}^z)^2 \tag{18}$$
$$+J_1(\mu_1^z + \mu_0^z)(S_{a,0}^z + S_{b,0}^z) + K_1((S_{a,0}^z \mu_1^z)^2 + (S_{a,0}^z \mu_0^z)^2 + (S_{b,0}^z \mu_1^z)^2 + (S_{b,0}^z \mu_0^z)^2) + \Delta((S_{a,0}^z)^2 + (S_{b,0}^z)^2)$$
$$+\Delta_1(\mu_1^z)^2 - h_H(S_{a,0}^z + S_{b,0}^z) - h_I \mu_1^z)] * g_{n-1}(\mu_1)$$

by inserting the eigenvalues of the operators and by using the equivalents of equations (15,16) the recursion relation has the following form

$$x_n = f1(x_{n-1}, y_{n-1}), \quad f_1(x,y) = \frac{a_1 + a_{11}x + a_{12}y}{b_0 + b_1 x + b_2 y} \tag{19}$$
$$y_n = f2(x_{n-1}, y_{n-1}), \quad f_2(x,y) = \frac{a_2 + a_{21}x + a_{22}y}{b_0 + b_1 x + b_2 y}$$

where the coefficients are easily calculated from equations (18).

The equations for total magnetic and quadrupole moments are expressed similar as [34].

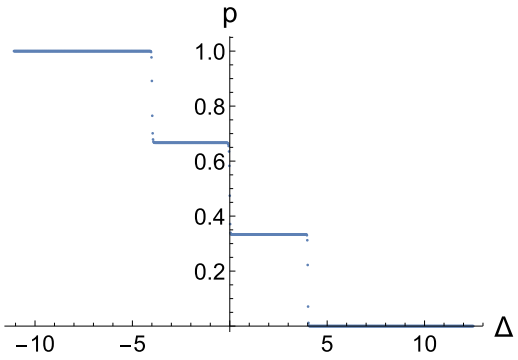

Figure 9. Quantum Ising-Heisenberg spin-1 quadrupole moment(p) for $J = 2, J_1 = 1, h = 0, T = 0.01$.

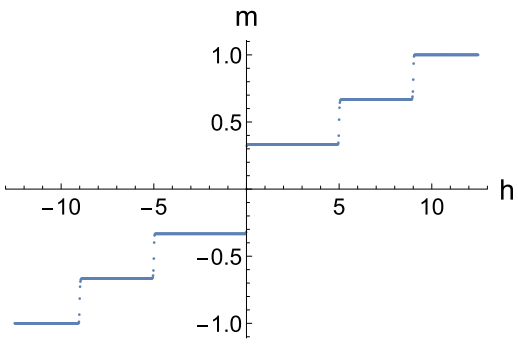

Figure 10. Quantum Ising-Heisenberg spin-1 magnetic moment(m) for $J = 2, J_1 = 1, \Delta = 1, T = 0.01$.

In the second part of this section we will focus on the thermodynamical equilibrium description of the spin-1 Ising/Ising-Heisenberg model on a diamond chain, by studying infinite-size systems. Lyapunov exponents have a crucial role in the study of "stability" or "instability"

of systems. Lyapunov exponents are the growth rate of an infinitesimal perturbation on a reference trajectory. The following values of maximal Lyapunov exponents can be observed during the investigation ($\lambda = max(\lambda_i)$).
$\lambda < 0$ negative Lyapunov exponents show that the system is dissipative or non-conservative. The systems with more negative values of Lyapunov exponent are more stable. If $\lambda = -\infty$ means that we have superstable fixed and superstable periodic points. $\lambda = 0$ corresponding to neutral fixed point. At this value of Lyapunov exponents the second-order phase transition takes place. $\lambda > 0$ corresponding to unstable and chaotic systems. In general case if we have a N dimensional map the $i-th$ Lyapunov exponent is calculated with the following equation

$$\lambda_i = \lim_{n\to\infty} \frac{\log H_i}{n}, \quad \mathbf{H} = J(x_0)J(x_1)...J(x_n) \tag{20}$$

where H_i is the $i-th$ eigenvalue of $\mathbf{H}$ and $J(x_k)$ is the Jacobian matrix of our N dimensional map after k iterations from the initial point x_0. In some cases when the eigenvalues of $\mathbf{H}$ are complex numbers and its reasonable to use $\mathbf{H}^{\dagger}\mathbf{H}$ ($\dagger$ denotes the transpose operator) instead of $\mathbf{H}$. In that case Lyapunov exponents will have $\lambda_i = \lim_{n\to\infty} \frac{\log H_i}{2n}$ form.

Superstable points are particularly interesting studying maximal Lyapunov exponent in classical and quantum cases. In this aspect the above mentioned models have many similarities as well as fundamental differences. There is a superstable point in the spin-1 Ising model at $h = 0$, $J = 2$, $J_1 = 1$, $T \to 0$ and $\Delta > 0$. By computational research it's shown that for many antiferromagnetic configurations there is a superstable point if $\Delta > 0$ which vanishes for $\Delta < 0$ configurations. Ising-Heisenberg models behavior is similar, many antiferromagnetic configurations have superstable points but unlike the Ising model here are two superstable points and they vanish if approximately $\Delta < -1.75$ (this point is for $h = 0$, $J = 2$, $J_1 = 1$ configuration). The fact that there is a magnetization plateau around supercritical points in the classical (see Figures 8, 11) and quantum (see Figures 10, 12) cases is of great importance.

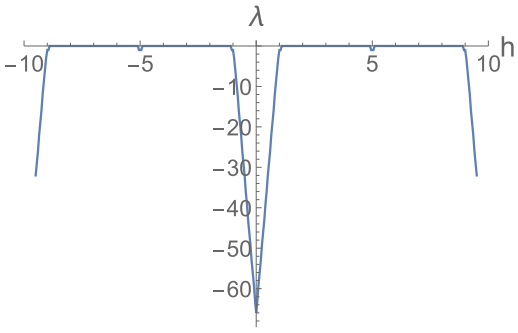

Figure 11. Classical Ising spin-1 maximal Lyapunov exponent for $J = 2, J_1 = 1, \Delta = 1, T = 0.03$.

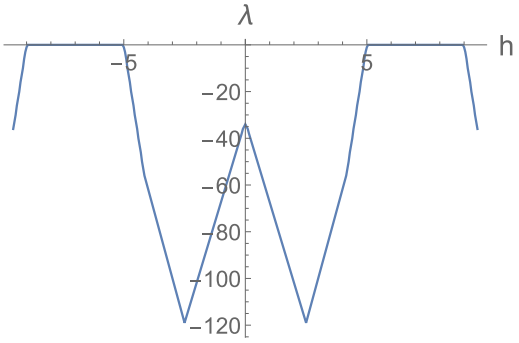

Figure 12. Quantum Ising-Heisenberg spin-1 maximal Lyapunov exponent for $J = 2, J_1 = 1, \Delta = 1, T = 0.03$.

5. Conclusions

In this paper we study symmetric IsingHubbard, spin-1 Ising and Ising-Heisenberg models on a diamond chain using transfer matrix and dynamical system methods for antiferromagnetic case. The behavior of the magnetization plateaus and thermal quantum entanglement are observed. It's detected the behavior of maximal Lyapunov exponent curves and superstable points connections with magnetization plateaus at $T \to 0$ in classical and quantum cases. It becomes exponentially more difficult to study the model with dynamical approach regarding

the case of $T < 0.01$, during calculations some elements become smaller than 10^{-1000}. Similar problems arise for greater values of J, J_1, Δ and h. This type of complications may justify the use of other non-standard approaches in the future.

Acknowledgments

This work was supported by MC-IRSES No. 612707 (DIONICOS) and CS MES RA in the frame of the Research Project no. SCS 15T-1C114 grants.

References

[1] Hida K 1994 *J. Phys. Soc. Jpn.* **63** 2359
[2] Ohanyan V R and Ananikian N S 2003 *Phys. Lett.* A v**307** 76
[3] Kikuchi H, Fujii Y, Chiba M, Mitsudo S, Idehara T, Tonegawa T, Okamoto K, Sakai T, Kuwai T and Ohta H 2005 *Phys. Rev. Lett.* **94** 227201
[4] Rule K C, Wolter A U B, Süllow S, Tennant D A, Brühl A, Köhler S, Wolf B, Lang M and Schreuer J 2008 *Phys. Rev. Lett.* **100** 117202
[5] Jeschke H et al. 2011 *Phys. Rev. Lett.* **106** 217201
[6] Kang J, Lee C, Kremer R K and Whangbo M-H, 2009 *J. Phys.: Condens. Matter* **21** 392201
[7] Ananikian N, Lazaryan H, Nalbandyan M 2012 *Eur. Phys. J.* B **85** 223
[8] Gu B and Su G 2007 *Phys. Rev.* A **75** 174437
[9] Takano K, Kubo K and Sakamoto H 2003 *J. Phys.: Condens. Matter* **15** 5979
[10] Čanová L, Strečka J and Jaščur M 2006 *J. Phys.: Condens. Matter* **18** 4967
[11] Rojas O, de Souza S M 2011 *Phys.Lett.* A **375** 1295
[12] Rojas O, de Souza S M and Ananikian N S 2012 *Phys. Rev.* E **85** 061123
[13] Nalbandyan M, Lazaryan H, Rojas O, de Souza S M and Ananikian N S 2014 *J. Phys. Soc. Jpn.* **83** 074001
[14] Konar S, Mukherjee P S, Zangrando E, Lloret F and Chaudhuri N R 2002 *Angew. Chem. Int. Ed.* **41** 1561
[15] Amico L, Fazio R, Osterloh A, Vedral V 2008 *Rev. Mod. Phys.* **80** 517
[16] Horodecki R, Horodecki P, Horodecki M, Horodecki K 2009 *Rev. Mod. Phys.* **81** 865
[17] Sachdev S 1999 *Quantum Phase Transition*(Cambridge: Cambridge University Press)
[18] Torrico J, Rojas M, de Souza S M, Rojas O and Ananikian N S 2014 *EPL* **108** 50007
[19] Ananikian N S , Ananikyan L N, Chakhmakhchyan L A and Rojas O 2012 *J. Phys.: Condens. Matter* **24** 256001
[20] Chakhmakhchyan L, Ananikian N, Ananikyan L and Burdík Č 2012 *J. Phys.: Conf. Series* **343** 012022
[21] Rojas O, Rojas M, Ananikian N S, de Souza S M 2012 *Phys. Rev.* A **86** 042330
[22] Abgaryan V S, Ananikian N S, Ananikyan L N, Hovhannisyan V 2015 *Solid State Commun.* **203** 5
[23] Abgaryan V S, Ananikian N S, Ananikyan L N, Hovhannisyan V 2015 *Solid State Commun.* **224** 15
[24] Torrico J, Rojas M, de Souza S M, Rojas O 2016 Zero temperature non-plateau magnetization driven by XY-anisotropy and magnetocaloric effect in Ising-XYZ diamond chain structure *Preprint* arXiv:1602.07279
[25] Jie Q and Bin Z 2015 *Chin. Phys.* B **24** 110306
[26] Ananikian N S and Dallakian S K 1997 *Physica* D **107** 75
[27] Akheyan A Z and Ananikian N S 1996 *J. Phys.* A **29** 721
[28] Avakian A R, Ananikyan N S and Izmailyan N Sh 1990 *Phys. Lett.* A **150** 163
[29] Ananikian N, Artuso R, Chakhmakhchyan L 2014 *Commun. Nonlinear Sci. Numer. Simul.* **19** 3671
[30] Ananikian N S, Ananikyan L N and Chakhmakhchyan L A 2011 *JETP Lett.* **94** 39
[31] Ananikian N, Ananikyan L, Artuso R, Lazaryan H 2010 *Phys. Lett.* A **374** 4084
[32] Ananikian N, Hovhannisyan V 2013 *Physica* A **392** 2375
[33] Lazaryan H, Nalbandyan M and Ananikian N 2016 *Int. J. Mod. Phys.* B **30** 1650135
[34] Hovhannisyan V V, Ananikian N, Kenna R 2016 *Physica* A **453** 116
[35] Wootters W K 1998 *Phys. Rev. Lett.* **80** 2245
[36] Vidal G and Werner R F 2002 *Phys. Rev.* A **65** 032314